JOURNAL OF AIRCRAFT
Vol. 29, No. 3, May–June 1992

Microwave Landing System Modeling with Application to Air Traffic Control Automation

M. M. Poulose*
Institut Teknologi, Bandar Seri Begawan 1929, Brunei

A model for evaluating the effects of scatterers on microwave landing systems (MLS) is presented and the feasibility of its incorporation into air traffic control (ATC) automation is discussed. The model is versatile enough to handle the effects of undulation, the roughness and the impedance of the terrain, and other scatterers commonly found in airport environments. Innovative techniques are used to reduce the computational burden which would enable the scattering effects on MLS position information to be evaluated in near-real time. This would permit the incorporation of the modeling scheme into ATC automation which would then adaptively delineate zones of reduced accuracy within the MLS coverage volume, and help establish safe approach and takeoff trajectories in the presence of terrain and other scatterers. The model is applied to several airport scenarios, and the results are discussed.

Introduction

SINCE aircraft about to land have very low margins of speed and altitude to effect a recovery in case of loss of control, accuracy of guidance information is crucial to safe and comfortable landing. The need for this accuracy is becoming even higher as air traffic densities are increasing at terminal areas and there is pressure to increase the landing rates. The microwave landing system (MLS) is a response to the need for greater traffic handling capacity, accuracy and versatility of landing guidance, and reduced susceptibility to disturbing effects of site reflections.[1-3] However, the MLS, which has gone through an extended period of development and proving and is at the beginning phase of operational installation, has the possibility of being affected by certain kinds of interference, especially because of the dense traffic that the system is expected to handle.

The effect of interference on MLS may be more critical than the currently used instrument landing system (ILS). This is because the MLS is designed to provide multiple approach corridors to aircraft. There is thus less margin for error in the MLS than the ILS in which errors become catastrophic only when they are so large as to affect obstruction clearance. A second reason for the sensitivity of MLS is its higher operating frequency which would make smaller scatterers appear electrically larger. Thus the effect of objects like parked or moving automobiles or aircraft, which are not significant at ILS frequencies, will be enhanced at the MLS frequencies.[4]

The experimental method of MLS evaluation has certain important drawbacks. Setting up the equipment and performing the experiment takes a long time and is very expensive. Another, and perhaps more serious, limitation of the experimental method is that it provides information on the MLS behaviour only for an existing site. If the site is not found suitable, the method cannot provide guidance regarding the nature and extent of site development necessary to make it acceptable. Air traffic control (ATC) automation[5,6] is another area where the insight into the MLS behaviour is crucial. Since MLS is designed to provide multiple approach corridors to aircraft, relatively small aberrations could enhance the probability of conflict among approaching aircraft. A priori knowledge about the course aberrations will, therefore, enable appropriate margins to be built into the ATC automation tool.

There is, thus, a strong motivation for research into analytical methods for site evaluation, preferably avoiding experimental procedures. Because of the availability of large computing power, such methods would be inexpensive, and they could predict the MLS behaviour for several assumed terrain shapes and scattering objects. A model developed by Evans et al.[7] is based on the Fresnel-Kirchoff diffraction formula[8,9] which is integrated over a rectangular region. In this method, the ground surface is divided into a number of triangular or rectangular plane surface elements, and the small scale roughness is treated using the Beckman-Spizzichino approximation.[10] This model mainly uses a combination of physical optics (PO) and geometric optics (GO) to obtain the desired accuracy within reasonable computation speed. However, in applying the PO method, the simplifying assumption is usually made that the ground currents in one area have no effect on the neighbouring areas. Such an assumption is necessary to determine the fields within reasonable computation time, but it implies that the electric fields radiated by the ground pass through any subsequent obstructions as if they do not exist.

Another MLS model developed by ITT Gilfillan[11] has used the geometric theory of diffraction (GTD) to determine the fields. However this model has made certain simplifying assumptions with regard to ray types and conductivity aspects to keep the computation time within reasonable limits.

This paper presents a powerful analytical approach for the determination of the quality of MLS performance in the presence of non-ideal scatterers based on an impedance uniform theory of diffraction (impedance UTD) model and a closed-form geometric method for ray tracing. This modeling choice is expected to increase the modeling accuracy with far less evaluation time and expense, given the low cost and high accessibility of modern computing systems. The model is applied to terrain geometries, and the results are compared with earlier results and measurements. Finally, the use of MLS scatter effect modeling in ATC automation is discussed.

System Features

The time reference scanning beam (TRSB) MLS system composition is shown in Fig. 1. It consists of forward azimuth, elevation, back azimuth, and flare equipment operating in the 5000 MHz carrier frequency band. The MLS uses two narrow beams which are scanned in an oscillatory manner in the azimuth and elevation sectors. At every position within the

Received April 11, 1990; revision received June 13, 1991; accepted for publication June 18, 1991.

*Department of Electrical and Electronics Engineering, P. O. Box 2909.

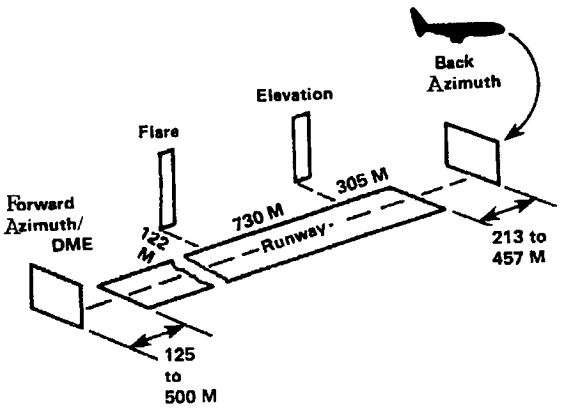

Fig. 1 TRSB MLS system composition.

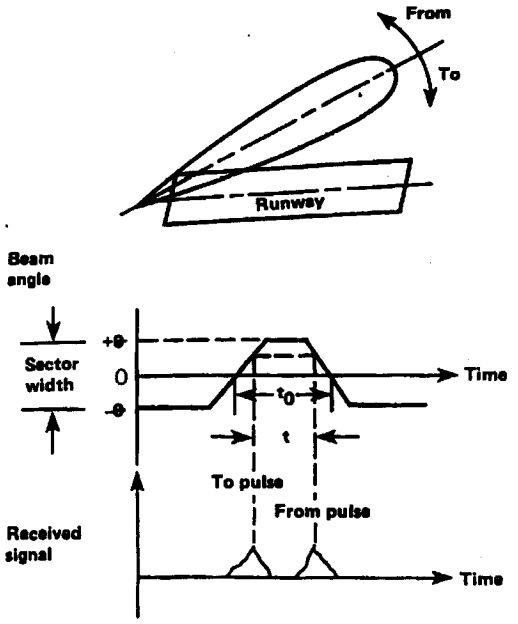

Fig. 2 Beam sweep angle as a function of time.

scan sector, an aircraft will receive two pulses from each beam corresponding to the to and fro scans. The aircraft derives its position within the coverage volume by measuring the time difference between these pulses pairwise. The azimuth scan uses a fan beam broad in the vertical plane and narrow in the horizontal plane. Similarly the elevation beam scans up and down using a fan beam broad in horizontal plane and narrow in vertical plane. Each beam scans its assigned sector (azimuth or elevation) at a constant sweep rate. There is a final dwell time (time of transit of the beam during which it exceeds the threshold level) at the end of each stroke. A schematic representation of beam sweep angle as a function of time is shown in Fig. 2. The same figure applies to both beams with different scales.

MLS Multipath Effects

The MLS has a more elaborate design than the ILS with the objectives of increasing the traffic handling capacity and reducing the site effects.[12] The beam configuration makes it possible for the MLS to cover a much larger sector than the ILS with a narrow beam. Further, the design of the radiation patterns of the MLS antennas is aimed to minimize the power radiated in the direction of terrain features, resulting in reduced site effects.[13]

There are, however, reasons that make the study of site effects important for the MLS. First, the standard terrain conditions assumed for the MLS may not be valid everywhere. For example, although the lower scanning limit of 1 deg for the vertical scan ensures that the elevation coverage beam stays clear of the ground at its lowest position, this may not be so if the ground has significant slope. Further, scattering due to sidelobes could have significant interfering effect.[14]

The error arising out of a multipath signal depends on its angular separation δ from the direct signal. The multipath signal at an angular coordinate different from the direct signal will result in the shifting of the centroids of the received beam shapes. Given the transmitter beamwidth θ and the amplitude ratio A_r, the in-beam multipath error, when δ is less than 1.5θ, can be in the order of $A_r\theta/2$.[15] When the level of the out-of-beam multipath compared to the direct signal remains higher for a sufficiently long time, it can result in significant error. This duration can be typically 5s, and the worst case error in such situations can be $A_r\theta$ times the sidelobe amplitude ratio.[15]

Theoretical Background

Early efforts at evaluating the electromagnetic fields in the presence of scatterers were based on physical optics.[16,17] In this method, fields are evaluated from assumed currents through a process of integration. This requires heavy computational effort and cannot model obstructions and shadow effects. Variants of this model, incorporating half-plane diffraction were next proposed, but these also suffered from limitations regarding the type of terrain and other scatterers handled.

The more recent modeling approaches have relied on ray theory. Since the size of the scatterers, and the significant features on it, are large compared to the operating wavelength, the scattering behaviour is expected to be close to optical in nature.[18] This makes a ray-theoretic approach a natural choice, and such an approach has been used predominantly in recent studies.[19,20] The simplest of such models considers only the direct rays from the antenna to the aircraft, and the rays reflected from the scatterers. The drawback of this model is that it predicts discontinuous fields due to shadow effects; this is against physical reality.

Perhaps the largest quantum jump in the search for accurate ray-theoretic field prediction around a wedge was contributed by J. B. Keller[21] through his geometric theory of diffraction (GTD) which considered diffracted rays in addition to reflected and direct rays. This theory predicted the field nearly everywhere with high accuracy except in two narrow sectors along reflection and shadow boundaries, where infinite fields (singularities) were predicted (Fig. 3).

More recent theories have been available to tackle the field singularity problem. Two well-known members of this class are the uniform theory of diffraction (UTD)[22,23] and uniform asymptotic theory (UAT).[24] These theories take different approaches to the determination of the diffraction coefficient, but each predicts a continuous and bounded field estimate. The perfectly conducting model does not take into account the surface roughness and impedance properties of the scatterer. These properties have been taken into account in the impedence UTD formulation[25] where the diffraction coefficient has been modified by introducing the Maliuzhinets function[26] (see Appendix).

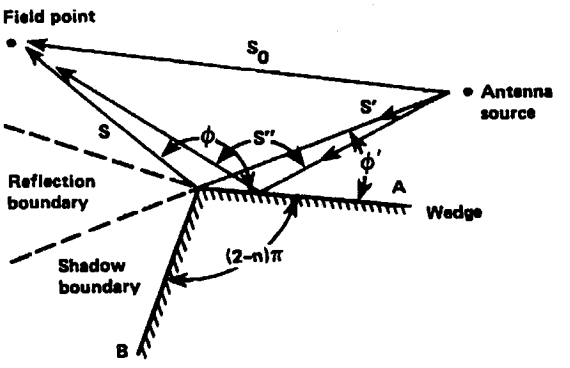

Fig. 3 Wedge parameters and ray geometry.

Modeling

All theories using the diffraction phenomenon, including the GTD, UTD, and impedance UTD assume a wedge as the basic element. Diffraction occurs at the edge between the two plane faces of the wedge. To be able to harness these theories for MLS modeling, the most convenient approach, therefore, is to visualize the terrain and other scatterers as a succession of plane surfaces, forming wedges pairwise (see Fig. 4). Such multi-plate models have been used in the recent past for scatter effect studies.[28-30]

A good way of arriving at a multi-wedge approximation is to obtain the terrain profile along a vertical plane parallel to the runway centreline and passing through the antenna location, to approximate the profile by straight-line segments, and finally to translate the line-segmented profile laterally to obtain the wedge structure. Clearly, the number of such planes required to model the terrain faithfully would depend on the extent of undulation present in the terrain and would be based on a compromise between accuracy and tractability.

Other factors that influence the scattering behaviour are the impedance and surface roughness of the scatterer. In locations, especially those involving dry and sandy soils, impedance effects cannot be neglected and must be built into the model. It is also possible to incorporate roughness effects into the model by using an equivalence relation which expresses the roughness in terms of an equivalent surface impedance which may be added to the inherent surface impedance.[27] The multi-wedge approximation, after incorporation of the surface impedance and roughness effects, constitutes the complete model of the terrain that is used to evaluate the site effects. Objects like hangars, buildings, etc. are also modeled in a similar way using the multiplate modeling approach. The multipath levels from aircraft surfaces such as the front and rear of the fuselage, leading and trailing edges of wings and engines are shown to be 15 dB below that of the fuselage and tail fin.[31] It is therefore assumed that the fuselage (main body) and the tail fin are the significant scatterers for MLS multipath effects and are considered in this work. For each aircraft position, a profile of the fuselage and tail fin is determined with respect to the antenna location for scattering computations.

Ray Tracing

The presence of multiple scatterers/wedges in the model means that the electromagnetic rays radiated from the antenna can reach an approaching aircraft through many possible paths. The first step in applying the ray-theoretic approach to the MLS problem is the process of ray tracing which involves the determination of all unblocked ray paths from each antenna element to the current position of the aircraft. In addition to the direct ray from the antenna to the aircraft, numerous rays will reach the aircraft after being scattered by the ground and other scatterers.

A ray striking the scatterer, modeled as multiple plates or wedges, may suffer reflection on a plate surface or diffraction at an edge. Rays emanating from an antenna element may reach the aircraft after either a single reflection or diffraction or a sequence of reflections and/or diffractions in any order. Accordingly, rays may be classified as singly reflected or diffracted rays or higher order rays such as reflected-reflected, reflected-diffracted, diffracted-reflected-diffracted, etc. A diffracted-reflected-reflected ray is shown in Fig. 5 as an example.

The order of a ray is the number of reflections and/or diffractions it undergoes before reaching the aircraft. The highest order of rays in general will be infinite. However, the contribution of rays will generally diminish with increase in their order.[30] For a multiwedge model, a large number of ray combinations involving many wedges/planes is possible, not all of which may exist in a given situation. Ray tracing to determine all possible rays is thus a complex exercise which has conventionally been carried out by a numerical search procedure. Such a procedure requires large computational effort and yields essentially approximate results. In this work, a systematic geometric method has been devised, along with the necessary computer programs, that generates exact solutions for the existence and location of all rays up to any specified order and tests for their existence.

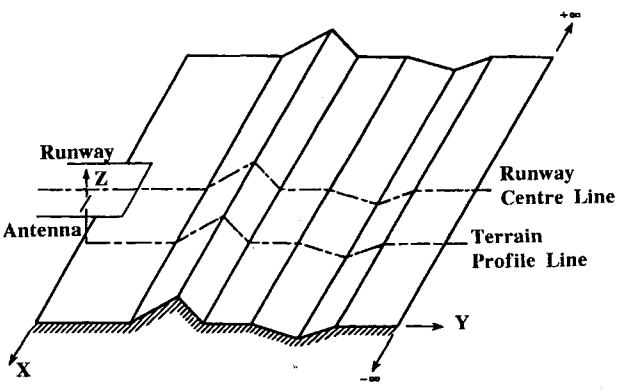

Fig. 4 Schematic of a multiwedge model of an airport terrain.

Results and Discussion

Accurate determination of the electromagnetic field at the aircraft location is an important step in the modeling. The diffraction from the edges of the wedges, as also reflection from the plane segments of the model, are dependent on the characteristics of the scatterer, particularly its impedance. While nearly all the earlier models assumed the terrain and other scatterers to be perfectly conducting, this model takes into account the impedance of the scatterers. Through an equivalence relationship, the surface roughness has also been taken into account. The ability to handle the surface undulation, surface roughness, and impedance, separately or simultaneously, makes the model both general and powerful.

Application to Experimental Site

To demonstrate the difference in fields computed by using the various modeling approaches, an experimental site[7] shown in Fig. 6 is used for computing the fields at different elevation angles. The site has both up-slopes and down-slopes and has several features that are common with airport terrains around the world. The curves in Fig. 7 show the computed power versus elevation angle for the actual C-band measurements[32] and the results obtained by Evans et al.[7] All the curves show a similar pattern, though the one obtained using the approach outlined here follows more closely the measured values. This may be due to the difference in the modeling approach and the use of accurate field estimation using impedance UTD.

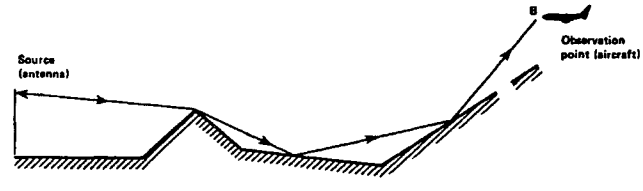

Fig. 5 A diffracted-reflected-reflected ray.

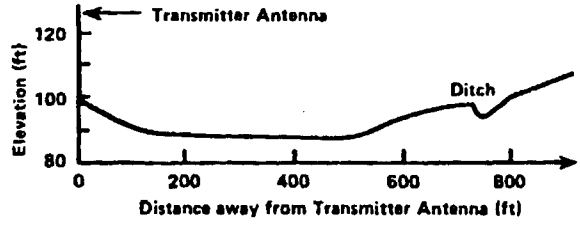

Fig. 6 Experimental site (Fort Devens, MA, golf course).

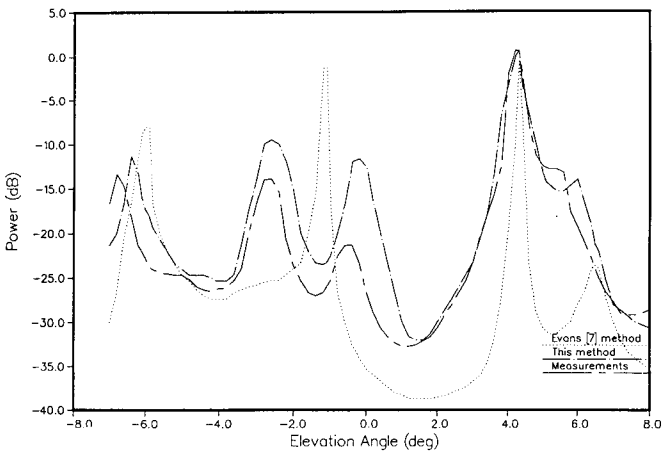

Fig. 7 Computed and measured power vs elevation angle.

Further, the model developed in this work tests for all rays of any order and combination. This means that the primary ray types (direct, reflected and diffracted) are combined in any order up to any level, and the model would automatically check for the existence of all possible combinations for the given antenna and aircraft location. Such a scheme ensures that the field contribution due to all possible unblocked ray paths are taken into account. However, all the curves demonstrate the presence of direct signal at 4.2 deg with two prominent specular returns.

Application of Hypothetical Airport Site

The international civil aviation organization (ICAO) has specified[33,34] a flight validation process for glideslope which includes a level run and a low level approach for measuring the vertical and structural characteristics of the glideslope. In the low-level approach the flight is along the nominal glideslope and the error in angle should ideally remain zero throughout. In practice, however, there will generally be a residual error whose prominent component is random, caused by navigational uncertainties, gusts, measurement inaccuracies, etc. The recorded error along the nominal glideslope approach is expressed in terms of statistical parameters which are used to determine the quality of the glideslope. The error in the case of MLS is required to be less than .001 deg. A hypothetical airport model shown in Fig. 8 with the elevation antenna located at a distance 450 ft offset from the runway centre line is now considered. The desired elevation angle is 3 deg. The ground elevation is up to about 8 ft with respect to the antenna mast base. A five-plate model has been used to model the terrain. The impedance model has been used for the field estimation. This permits the inclusion of the effects of surface roughness and surface impedance, in addition to the effect of ground undulation. The surface roughness parameter for the terrain is assumed to be 0.3, and the surface impedance of the dry sandy terrain is 3-j0.06 Ω (per square). The computed elevation error for a low level approach is shown in Fig. 9. The maximum error is more than 0.029 deg. This high degree of error can be attributed to the upslope in the terrain geometry considered here. Several simulations were carried out with different terrain geometries, and it has been observed that only terrain undulations within 960 ft from the antenna contribute significantly to the multipath effects. Beyond 960 ft, the error is observed to be less than 0.01 deg. Further, the sloping terrain within the above region is responsible for maximum error.

Application to Aircraft in ATC Environment

The B 747 aircraft is known to be extreme in terms of fuselage and tail fin sizes, and therefore scattering from this aircraft is expected to induce maximum error. Hence in this model, a 747 aircraft has been simulated to the beginning of the runway. The error vs distance is shown in Fig. 10. It has

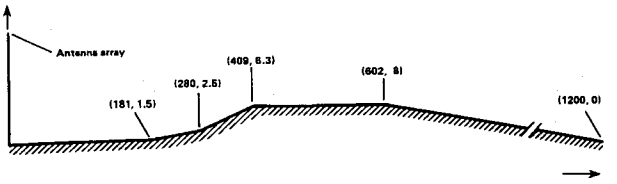

Fig. 8 Five-segment approximation of hypothetical airport site. Coordinates are in feet (not to scale).

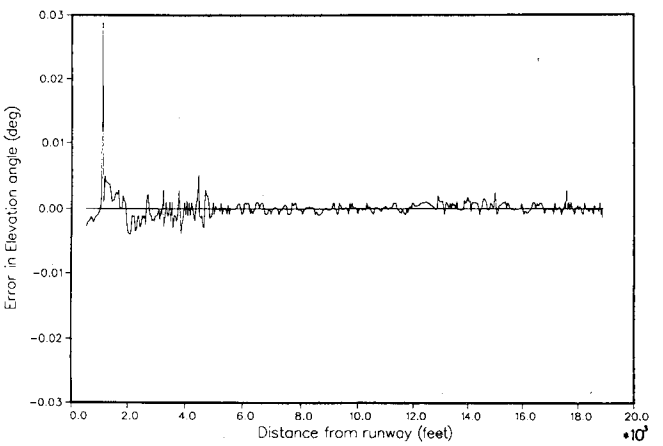

Fig. 9 Computed error vs elevation angle for the airport in Fig. 8 for a low-level approach.

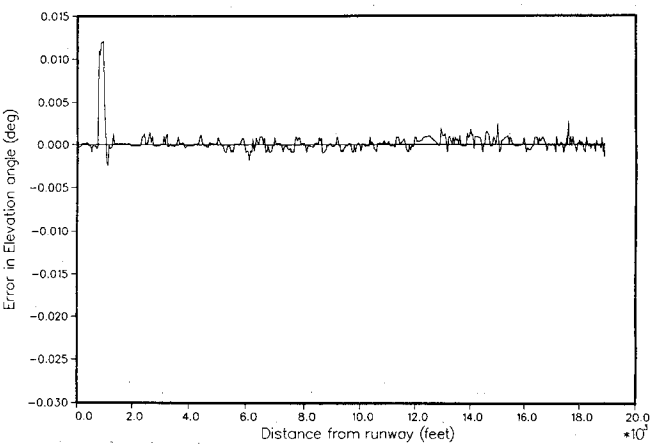

Fig. 10 Computed error in elevation angle vs distance for a low-level approach when a B 747 aircraft is modeled at the end of the runway.

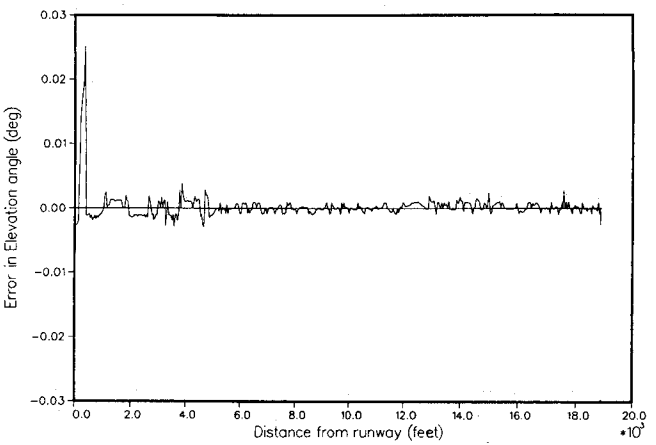

Fig. 11 Computed error in elevation angle vs distance for a low-level approach when the B 747 aircraft is at an offset distance of 500 ft and 150 ft to the front of elevation antenna.

been noticed that the 747 aircraft has resulted only in an error of 0.012 deg for an aircraft in the final approach at a distance of about 900 ft from the instrument runway. This result indicates that the movement of aircraft on the runway is not likely to affect the performance of the elevation equipment. Another simulation was carried-out by modeling an aircraft at a distance of 500 ft from the edge of the runway and is 150 ft to the front of the elevation antenna. This has resulted in an error of more than 0.025 deg (Fig. 11) which may be quite unacceptable. Thus taxi tracks, roads, etc. within 500 ft from the runway and in front of the elevation antenna are likely to cause unacceptable errors.

Use of MLS Scatter Effect Modeling in ATC Automation

As already mentioned, since the MLS (unlike ILS) is designed to provide multiple approach corridors to aircraft, errors arising from multipath effects could enhance the probability of conflict among approaching aircraft. To minimize such conflict probability, it is desirable to build MLS scatter effects into the ATC automation scheme so that any perceptible aircraft course deviation due to the scattering environment of the MLS that may lead to a potential conflict is available as an input for the automation tool.

In incorporating the MLS model into an automated ATC tool, the scattering environment of the MLS may be divided into two parts. One part consists of the "fixed" scatterers such as terrain features, hangars, antenna masts, and other airport structures in the MLS influence area. A map of such scatterers can be obtained, and the course aberrations due to the scatterers computed, for each MLS installation in the ATC network. Since such a computation can be carried out off-line, a full-fledged and accurate analysis may be employed to do the analysis, using the impedance UTD method in conjunction with an accurate terrain model using a large number of plates/wedges. Further, field evaluation may be conducted at a large number of closely spaced points over the MLS coverage volume, and the vector fields at those points may be stored as a look-up table in computer memory for combination with other field contributions, such as those shown below.

The second part of the scattering environment consists of the moving (or movable) scatterers such as aircraft parked, taxiing, or flying in the MLS influence volume, parked or moving vehicles, or other temporary structures. The effects of scattering from these bodies would have to be modeled for dynamic, real-time evaluation. This requires the use of relatively simple algorithms. Considerable simplicity results from the fact that these effects need be computed only at a few discrete points corresponding to the current locations of the aircraft being guided by the MLS. Further simplicity may be attained by assuming the scatterers to be fully conducting, which is valid for aircraft, vehicles, and metal hangars. This permits the use of the simpler UTD-based field computation, which results in several-fold savings in computational efforts compared to the more elaborate impedance UTD method. To a first order, the effect of each "temporary" scatterer may be considered separately and vectorially added to the field due to the fixed scatterers (retrieved from the computer memory) to provide an estimate of the total aberration due to the scattering environment. The relatively weak second-order effects due to the rays bouncing among the scatterers and between the scatterers and the terrain would require too much computation for cost-effective real-time implementation, and is not recommended at the present time.

The results of the scatterer-effect simulation would appear as a certain inaccuracy in position location of aircraft that utilize the MLS information for that purpose. The automated ATC system could thus take this error into account in its conflict detection and resolution algorithms. Thus, the separation criteria between aircraft at each particular zone within the MLS coverage volume should be enlarged to take into account the additional position inaccuracy due to scatter effects. A good criterion to compound the stipulated separation distance and the expected error due to scatter effects is to add them in a root-mean-square (rms) sense, since the actual position of the aircraft within the allocated volume and the sense of the scatter-induced errors are well-approximated as uncorrelated random variables.

Model Validation

Further studies in this area include a statistical estimation, by experimental means, of the accuracy of the MLS guidance in the presence of scattering effects by comparing the position information of the MLS with other position location devices such as the radar and the aircraft's inertial navigation system. Such an analysis will validate the accuracy of the modeling approach and pave the way for its successful integration into the ATC automation process.

Conclusion

An attempt has been made in this paper to present a perspective of the important problem of the effect of site and other scatterers on MLS and to outline the developments relating to the evaluation of multipath effects on the system performance. Details of the developments and sample results are provided. It has been shown that, with a proper combination of modeling, ray tracing, and powerful field evaluation techniques, it is possible to evaluate MLS multipath effects quite realistically. The results of the simulations carried out in this study show that aircraft in front of the elevation antenna induce unacceptable errors in elevation angle. While this study has simulated sample results for terrain irregularities and scatterers like aircraft, more full-run simulations are necessary to evaluate the effects in a variety of situations encountered in actual ATC operations. The formation, including the ray-tracing algorithm is generally capable of handling any scatterer, ray order, and impedance. This provides freedom to handle any airport situation, as well as other radio communication problems involving multipath. The major bottleneck in the use of analytical methods for scatter effect modeling hitherto has been the relative inaccuracy and computation-intensiveness of the method. This paper has pointed out that such constraints have now been largely removed, and the method is versatile enough to handle all types of scatterers encountered in practice. The accuracy, versatility, speed, and cost-effectiveness of the method is expected to make a significant practical contribution to the quality of ATC automation.

Acknowledgments

This work was done while the author held a NRC Research Associateship at the Aircraft guidance and Navigation Branch, NASA Ames Research Center. The author wishes to acknowledge the guidance and support received from Leonard Tobias during the course of this work. Thanks are also due to Heinz Erzberger, Asst. Branch Chief, and Dallas Denery, Branch Chief, for their encouragement. The author is also grateful to Haji Mustafa bin Abu Bakar, Director, Institut Teknologi Brunei, for the facilities afforded to him during the revision of this paper.

Appendix: Field Computation

According to GTD, the total field at an observation point is the sum of the geometric optics (GO) and diffracted fields and can be represented as (see Fig. 3)

$$E^t_{s,h} = E^g_{s,h} + E^d_{s,h}$$

$$= E_0 \left[\frac{e^{-jks_0}}{s_0} \mp \frac{e^{-jks''}}{s''} + \frac{e^{-jks'}}{s'} D_{s,h} e^{-jks} A_d \right] \qquad \text{(A1)}$$

where the diffraction coefficient $D_{s,h}$ and the divergence factor A_d are given by Keller[21]

$$D_{s,h} = \frac{-e^{-j\pi/4}\sin\frac{\pi}{n}}{n\sqrt{2\pi k}\sin\beta_0}\cdot\left[\frac{1}{\cos\frac{\pi}{n}-\cos\frac{\beta-}{n}} \mp \frac{1}{\cos\frac{\pi}{n}-\cos\frac{\beta+}{n}}\right] \quad \text{(A2)}$$

and

$$A_d = \frac{s'}{s'(s+s')} \quad \text{(A3)}$$

Equation (A3) is not valid in transition regions in the vicinity of shadow and reflection boundaries where it predicts infinite fields. The above drawback of the GTD has been overcome by the two uniform theories. In the UTD,[22] the diffraction coefficient in equation (A3) is modified by introducing Fresnel and cotangent functions and is given by

$$D_{s,h} = \frac{-e^{-j\pi/4}}{2n\sqrt{2\pi k}\sin\beta_0}\left\{\cot\left(\frac{\pi+\beta^-}{2n}\right)F(kLa^+\beta^-) + \cot\left(\frac{\pi-\beta^-}{2n}\right)F(kLa^-\beta^-) \pm \left[\cot\left(\frac{\pi+\beta^+}{2n}\right)F(kLa^+_+\beta^+) + \cot\left(\frac{\pi-\beta^+}{2n}\right)F(kLa^-_+\beta^+)\right]\right\} \quad \text{(A4)}$$

where

$$F(x) = 2j|\sqrt{x}|e^{jx}\int_{|\sqrt{x}|}^{\infty} e^{-t^2}\,dt \quad \text{(A5)}$$

and

$$a^{\pm}_{\pm} = 2\cos^2\left(\frac{2n\pi N^{\pm}_{\pm}-\beta^{\pm}}{2}\right) \quad \text{(A6)}$$

$N^{\pm}_{\pm}$ = integers which nearly satisfy the following equations:

$$2\pi n N^{+}_{\pm} - \beta^{\pm} = \pi \quad \text{(A7)}$$

$$2\pi n N^{-}_{\pm} - \beta^{\pm} = -\pi \quad \text{(A8)}$$

and

$$\beta^{\pm} = \phi \pm \phi' \quad \text{(A9)}$$

The distance parameter for spherical wave incidence is given by

$$L = \frac{ss'}{s+s'}\sin^2\beta_0 \quad \text{(A10)}$$

When the observation point moves away from the reflection and shadow boundaries, equation (A5) is reduced to (A3). Under this situation, the observation point is said to be outside the transition regions.

In UAT the diffracted field E^d is as in equation (A2). The modified GO field E^{q0} is given by[24]

$$E^{s0} = [F(\zeta^i) - \hat{F}(\zeta^i)]E^i + [F(\zeta^r) - \hat{F}(\zeta^r)]E^r \quad \text{(A11)}$$

where

$$F(x) = \frac{e^{-j\pi/4}}{\sqrt{\pi}}\int_x^{\infty} e^{it^2}\,dt \quad \text{(A12)}$$

$$\hat{F}(x) = \frac{1}{2x\sqrt{\pi}}e^{j(x^2+\pi/4)} \quad \text{(A13)}$$

$$\zeta^i = \mp\sqrt{(k)}|(s'+s-s_0)^{1/2}| \quad \text{(A14)}$$

and

$$\zeta^r = \mp\sqrt{(k)}|(s'+s-s'')^{1/2}| \quad \text{(A15)}$$

where the positive and negative signs correspond to the shadow and lit regions respectively.

The perfectly conducting model does not take into account the surface roughness and impedance properties of the scatterer. The diffraction coefficient D_s, h in the case of impedance formulation has been shown to be[25]

$$D_{s,h} = \frac{-e^{-j\pi/4}}{n\sqrt{2\pi k}\Omega^{s,h}\phi'}\left\{\Omega^{s,h}(\phi+\pi)\left[\cot\left(\frac{\pi+\beta^-}{2n}\right)\cdot F(kLa^+\beta^-) - \cot\left(\frac{\pi+\beta^+}{2n}\right)F(kLa^+_+\beta^+)\right] + \Omega^{s,h}(\phi-\pi)\left[\cot\left(\frac{\pi-\beta^-}{2n}\right)F(kLa^-\beta^-) - \cot\left(\frac{\pi-\beta^+}{2n}\right)F(kLa^-_+\beta^+)\right]\right\}$$

where

$$\Omega^{s,h}(\alpha) = M(-\alpha+\pi/2-\theta^{s,h}_B).M(-\alpha-\pi/2+\theta^{s,h}_B)\cdot M(-\alpha+n\pi-\pi/2+\theta^{s,h}_A)\cdot M(-\alpha+n\pi+\pi/2-\theta^{s,h}_A) \quad \text{(A16)}$$

with the Maliuzhinets' function $M(\alpha)$ defined as[26]

$$M(\alpha) = \prod_{n'=1}^{x}\prod_{m'=1}^{x}\cdot\left[1-\left(\frac{\alpha}{n\pi(2n'-1)+(\pi/2)(2m'-1)}\right)\right]^{(-1)^{m'+1}} \quad \text{(A17)}$$

and

$$\theta_s = \sin^{-1}(\varepsilon_r - \cos^2\phi')^{1/2} \quad \text{(A18)}$$

$$\theta_h = \sin^{-1}[(\varepsilon_r - \cos^2\phi')^{1/2}]\varepsilon_r \quad \text{(A19)}$$

The subscripts A and B refer to the two faces of the wedges in Fig. 3, and the superscripts s and h correspond to soft and hard boundary conditions on the wedge surface.

References

[1]DOT/NASA/DOD Planning Group, "National Plan for the Development of MLS," AD 733268, 1971.

[2]Special issue on MLS, *IEEE AES Systems Magazine*, Vol. 5, 1990.

[3]Poulose, M. M., "Terrain Modeling for Microwave Landing System," *IEEE Transactions on Aerospace and Electronic Systems*, Vol. 27, No. 3, 1991, pp. 1–9.

[4]Mahapatra, P. R., and Poulose, M. M., "Evaluating ILS and MLS sites without Flight Tests," *Journal of Navigation*, Vol. 42, No. 2,

1989, pp. 278–290.
[5]Tobias, L., Volckers, U., and Erzberger, H., "Controller Evaluations of the Descent Advisor Automation Aid," NASA TM-102197, 1989.
[6]Erzberger, H., and Nedell, W., "Design of Automated System for Management of Arrival Traffic," NASA TM-102201, 1989.
[7]Evans, J. E., Capon, J., and Shnidman, D. A., "Multipath Modeling for Simulating the Performance of the Microwave Landing System," *The Lincoln Laboratory Journal,* Vol. 2, No. 3, 1989, pp. 459–474.
[8]Goodman, J. W., *Introduction to Fourier Optics,* McGraw-Hill, New York, 1954.
[9]Sommerfeld, A., *Optics,* Academic Press, New York, 1956.
[10]Beckmann, P., "Scattering by Composite Rough Surface," *IEEE Proceedings*, Vol. 53, 1965, pp. 1012–1016.
[11]ITT, Gilfillan., "Microwave Landing System," Phase 1 Rept., 1972.
[12]Radio Technical Commission for Aeronautics (RTCA), "A New Guidance System for Approach and Landing," RTCA DO-148, 1970.
[13]Sebring, J. R., and Ruth, J. K., "MLS Scanning Beam Antenna Implementation," *The Microwave Journal,* Vol. 1, 1974, pp. 41–46.
[14]Mahapatra, P. R., and Poulose, M. M., "A Fast and Low Cost Validation Technique for ILS and MLS," IEEE Position Location and Navigation Symposium, Las Vegas, 1990.
[15]Evans, J. E., Burchsted, R. B., Capon, J., Orr, R. S., Shnidman, D. A., and Sussman, S. M., "MLS Multipath Studies," Lincoln Lab. Project Report ATC 63, 1976.
[16]Morin, S., Newsom, P., Kahn, D., and Jordan, L., "ILS Performance Prediction," Transportation System Center FAA-RD-74-157B, 1974.
[17]Ramakrishna, S., and Sachidananda, M., "Calculating the Effect of Uneven Terrain on Glidepath Signals," *IEEE Transaction on Aerospace and Electronic Systems,* Vol. AES, No. 3, 1974, pp. 380–384.
[18]Cornbleet, S., "Geometrical Optics Reviewed," *IEEE Proceedings,* Vol. 71, 1983, pp. 471–529.
[19]Luebbers, R., Ungvichian, V., and Mitchel, L., "GTD Terrain Reflection Model Applied to ILS Glideslope," *IEEE Transactions on Aerospace and Electronic Systems,* Vol. AES 8, No. 1, 1982, pp. 11–19.
[20]Poulose, M. M., Mahapatra, P. R., and Balakrishnan, N., "Estimation of ILS Glideslope in the Presence of Terrain Irregularities," *Journal of the Institution of Electronics and Telecommunication Engineers (India),* Vol. 33, No. 1, 1987, pp. 22–29.
[21]Keller, J. B., "Geometrical Theory of Diffraction," *Journal of the Optical Society of America,* Vol. 52, 1962, pp. 116–130.
[22]Kouyoumjian, R. G., and Pathak, P. H., "A Uniform Theory of Diffraction for an Edge on a Perfectly Conducting Surface," *IEEE Proceedings,* Vol. 62, 1964, pp. 1448–1461.
[23]Tiberio, R., and Kouyoumjian, R. G., "A Uniform GTD Analysis of Diffraction by Thick Edges and Strips Illuminated at Grazing Incidence," *International Symposium Digest, Antenna and Propagation,* Univ. of Maryland, 1978.
[24]Ahluwalia, D. S., Lewis, R. M., and Boersma, J. M., "Uniform Asymptotic Theory of Diffraction by a Plane Screen," *SIAM Journal of Applied Mathematics,* Vol. 16, No. 4, 1968, pp. 783–807.
[25]Poulose, M. M., and Mahapatra, P. R., "ILS Glideslope Evaluation for Imperfect Terrain," *IEEE Transactions on Aerospace and Electronic Systems,* Vol. AES 24, No. 2, 1988, pp. 1886–191.
[26]Maliuzhinets., "Excitation, Reflection and Emission of Surface Waves from a Wedge with Given Face Impedances," *Soviet Physics, Dokhladv,* Vol. 3, 1958, pp. 752–755.
[27]Poulose, M. M., Mahapatra, P. R., and Balakrishnan, N., "Accurate Prediction of Terrain Undulation and Roughness Effects in Radiating Systems," *Proceedings of the IEEE International Conference on Antennas and Communications,* Montreal, Canada, 1986.
[28]Brein, T., "Multipath Analysis of ILS Glidepath," ELAB, Trondheim, Norway, N 7034, 1979.
[29]Poulose, M. M., Mahapatra, P. R., and Balakrishnan, N., "Terrain Modelling of Glideslope for Instrument Landing System," *IEE Proceedings,* Sec. H, Vol. 34, No. 3, 1987, pp. 275–279.
[30]Poulose, M. M., Mahapatra, P. R., and Balakrishnan, N., "Computer Aided ILS Site Evaluation is Deemed Practical," *ICAO Bulletin,* Vol. 48, No. 9, 1986, pp. 36–39.
[31]Krispin, J. W., and Siegel, K. S., *Methods of Radar Cross-Section Analysis,* Academic Press, New York, 1968.
[32]Sun, D. F., "Experimental Measurements of Low Angle Ground Reflection Characteristics at L and C Bands for Irregular Terrain," Lincoln Lab. ATC-107, 1982.
[33]International Civil Aviation Organization (ICAO), "International Standards and Practices," Annexure 10, Montreal, Canada, 1968.
[34]International Civil Aviation Organization (ICAO), "Manual on Testing of Radio Navigational Aids," Annexure 11, Montreal, Canada, 1973.